THE JOURNAL OF PHYSICAL CHEMISTRY B

Article

pubs.acs.org/JPCB

Structural Properties of CHAPS Micelles, Studied by Molecular Dynamics Simulations

Fernando E. Herrera,*[,†] A. Sergio Garay,[†] and Daniel E. Rodrigues[†,‡]

[†]Departamento de Física, Facultad de Bioquímica y Ciencias Biológicas, Universidad Nacional del Litoral (UNL), Ciudad Universitaria, 3000 Santa Fe, Argentina

[‡]INTEC (CONICET-UNL), Güemes 3450, 3000 Santa Fe, Argentina

Supporting Information

ABSTRACT: Detergents are essential tools to study biological membranes, and they are frequently used to solubilize lipids and integral membrane proteins. Particularly the nondenaturing zwitterionic detergent usually named CHAPS was designed for membrane biochemistry and integrates the characteristics of the sulfobetaine-type detergents and bile salts. Despite the available experimental data little is known about the molecular structure of its micelles. In this work, molecular dynamics simulations were performed to study the aggregation in micelles of several numbers of CHAPS ($\leq$18) starting from a homogeneous water dilution. The force field parameters to describe the interactions of the molecule were developed and validated. After 50 ns of simulation almost all the systems result in the formation of stable micelles. The molecular shape (gyration radii, volume, surface) and the molecular structure (RDF, salt bridges, H-bonds, SAS) of the micelles were characterized. It was found that the main interactions that lead to the stability of the micelles are the electrostatic ones among the polar groups of the tails and the OH's from the ring moiety. Unlike micelles of other compounds, CHAPS show a grainlike heterogeneity with hydrophobic micropockets. The results are in complete agreement with the available experimental information from NMR, TEM, and SAXS studies, allowing the modeling of the molecular structure of CHAPS micelles. Finally, we hope that the new force field parameters for this detergent will be a significant contribution to the knowledge of such an interesting molecule.

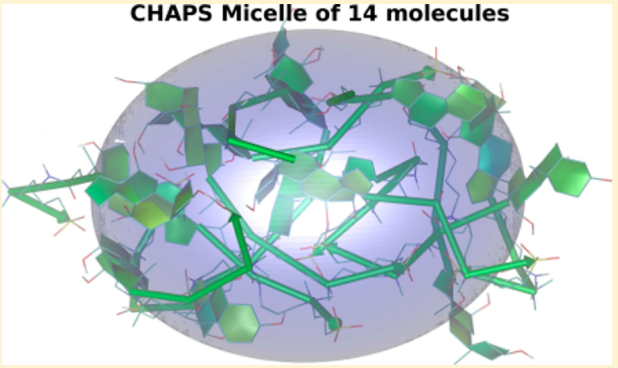

1. INTRODUCTION

Detergents are essential tools in the study of biological membranes. They are frequently used to solubilize lipids and integral membrane proteins, and to evaluate the strength of interaction of the membrane components.[1,2] The nondenaturing zwitterionic detergent, commonly called CHAPS (3-[(3-cholamidopropyl)dimethylammonio]-1-propanesulfonate), was originally designed for membrane biochemistry combining the characteristics of the sulfobetaine-type detergents and bile salts.[3] The characteristics that make this detergent different from the traditional ones are that it has a steroid structure with a convex side (β-plane or back) and a concave side (α-plane or face) on which there are 3 hydrophilic hydroxyl groups.[4,5] This peculiar distribution of its polar groups may result in an aggregation pattern and a micellar structure much different from those of other synthetic surfactants.[4]

Figure 1 shows the 2D structure diagram of a CHAPS molecule. It is composed of a hydrophilic "chain" group and a hydrophobic/hydrophilic "cholic" group (since it is a zwitterionic derivative of cholic acid). The first one is composed of an amide group, a dimethylammonium group, and the propene-sulfonate group. The configuration of the hydroxyl groups gives to the molecule a hydrophilic side while the other side remains hydrophobic due to the steroid nucleus (α and β planes). It has been proposed that these hydrophobic and hydrophilic faces are responsible for the aggregation behavior and surface configuration of the molecules.[6] This unique structure may lead CHAPS to an atypical aggregation behavior. It has been proposed that there are two types of

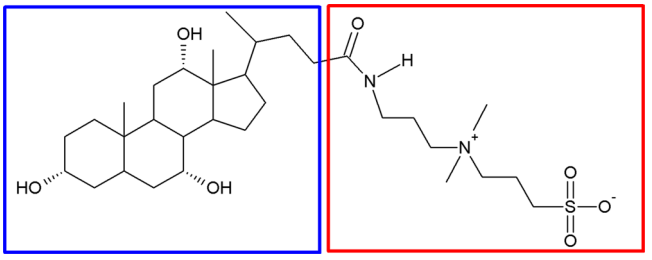

Figure 1. 2D structure diagram of a CHAPS molecule with the atom names included. The hydrophilic "chain" group and the hydrophobic/hydrophilic "cholic" group are marked in red and blue respectively.

Received: February 18, 2014
Revised: March 20, 2014

 © XXXX American Chemical Society dx.doi.org/10.1021/jp501729s | J. Phys. Chem. B XXXX, XXX, XXX–XXX

micelle aggregation which depend on CHAPS concentration, one at a critical micellar concentration (cmc) of 4−11 mM and the other at higher concentration (32.6[4]). The aggregation number estimated for CHAPS under the conditions of the first one are between 4 and 14,[7] which are included in the range we study in this work. Many previous experimental studies have appealed to structural models of the CHAPS micelles to explain their spectroscopic results.[4,5] These structural model proposals are based on some intuitive arguments about the hydrophilic/hydrophobic nature of the molecular moieties. Nevertheless none of them have been proved to be energetically consistent.

In this work we have used molecular dynamics simulations to study the aggregation process and the structural properties of CHAPS micelles with several numbers of molecules ($n \leq 18$). Molecular dynamics simulations have been proven to be useful to understand the molecular structure and dynamics of micelles for other species (octyl glucoside,[8,9] SDS,[10] phospholipids and bile salts,[11,12] OmpX/DHPC,[13] sulfobetaine,[14] dodecylphosphocholine,[15] etc). Nevertheless, to the best of our knowledge, this is the first report of the use of molecular dynamics simulations to study the CHAPS detergent and its aggregation in micelles. In this context, this work will present the developed interaction parameters for the molecule and some results which validate them against experimental data. The results allow us to obtain a model of the molecular structure of the CHAPS micelles to interpret the experimental information. As discussed bellow, the presented force field parameters are appropriate to be used in conjunction with the GROMOS 53a6 parametrization for other molecules.

2. METHODS

2.1. Parameter Development. In the first part of this work we developed the force field parameters for the CHAPS molecule, since there are not yet any published for this molecule.

The charge groups were defined according to the functional groups involved in the molecule. Atomic charges were obtained using the AM1BCC semiempirical calculations for the propenesulfonate group (with a total net charge of −1.0 e.u.), the charges for the dimethylammonium group were extracted from Berger's parametrization of the lipids choline group,[16] the charges for the amide group were obtained from an amide group of G53A6 force field,[17] and finally, the charges for the cholic group were extracted from the parameter of cholesterol published elsewhere.[18] The bonded parameters were obtained from the PRODRG server[19] and from the Automatic Topology Builder server,[20,21] both giving the same set of bonded parameters. Atom types and nonbonded parameters were assigned accordingly to the G53A6 gromos force field.[17] It should be noticed that the set of parameters obtained for the CHAPS molecule is completely compatible with the gromos G53A6 force field and it could also be used in combination with any force field parameters for other molecules. The complete set of parameters could be downloaded as Supporting Information.

2.2. Molecular Dynamics Simulations. All molecular dynamics (MD) simulations were performed using the Gromacs package version 4.5.[22−24] A direct cutoff for nonbonded interactions of 1 nm and particle mesh Ewald for long-range electrostatics were applied.[25] Berendsen[26] baths were used to couple the simulation boxes with an isotropic pressure of 1 atm and to the reference temperature. The CHAPS and WATER molecules were coupled to separate Berendsen thermostats with a relaxation time of 0.1 ps. All bond lengths were constrained using the LINCS algorithm[27] whereas the SETTLE algorithm[28] was used for water molecules. All the systems were solvated with SPC water molecules.[29] The time step in all the simulations was set to 2 fs.

2.3. Molecular Dynamics Protocol. The CHAPS molecules to be simulated (n = 1, 2, 4, 6, 8, 10, 12, 14, 16, and 18) were located at random in a truncated octahedral simulation box with around 10000 to 14000 water molecules. We use the following protocol to obtain unbiased initial conformations of each simulated system. The protocol consist of a three stage simulated annealing: (i) temperature rise from 298 to 400 K in 200 ps; (ii) constant high temperature step at 400 K by 800 ps; and (iii) cooling step to 298 K in 1 ns, followed by an equilibration phase of at least 30 ns (in one system with 18 molecules the equilibration phase took almost 80 ns), and finally a production step of 20 ns. To explore the dispersion of the analyzed properties due to different initial conditions, two independent systems were simulated for each number of molecules; they were obtained by starting the cooling stage at two different times of the high temperature period (400 ps and 800 ps). It is remarkable that after the simulated annealing protocol and before the equilibration stage the micelles were already formed in almost all systems. The number of CHAPS molecules simulated in the different systems of our study covers the range determined for the aggregation number in micelles of CHAPS using SAXS with concentration in the range 10 mM to 150 mM.[30] It is also worth noticing that the final CHAPS concentration for each system (e.g., 55.3 mM for 12 CHAPS system) is already above the second critical micelle concentration (CMC: 32.3 mM) proposed in some studies,[4] although the total number of molecules on each simulation do not allow for the formation of a second aggregation shell, as it is speculated in those works.[6]

All trajectories were analyzed using the standard tools from the Gromacs package and custom tcl/tk scripts in the VMD environment.[31] Different properties were calculated for each of the simulated systems along the trajectory (radius of gyration, radial distribution functions, solvent accessible surface area, etc). Temporal averages were calculated in all the cases along the production stage (the last 20 ns of simulation). The number of hydrogen bonds was calculated based on an angle acceptor−donor−hydrogen cutoff of 30 degrees and a distance donor−acceptor cutoff of 3.5 Å. A salt bridge was defined if the distance between the charged atoms that participate in the interaction is lower than 4.5 Å.

Additionally, the radius of gyration of the micelles was measured not only to quantify the overall shape of the micelles but also to evaluate the arrival to the production stage of each simulation. Therefore, a system was considered to be equilibrated when no further changes are found on the average principal components of the gyration radii and therefore in the micelle shape.

3. RESULTS

The simulated systems were chosen in order to explore different aggregation number on micelles.[4,7,30] We start by analyzing the behavior of one CHAPS molecule in water to explore its conformational space and test the developed force field parameters. Also the case of two molecules was considered with this purpose and to explore the basic intermolecular interactions. Then higher aggregation numbers of CHAPS molecules were considered and its micelle properties analyzed.

dx.doi.org/10.1021/jp501729s | J. Phys. Chem. B XXXX, XXX, XXX−XXX

3.1. Molecular Dynamics of an Isolated CHAPS Molecule. The behavior of one CHAPS molecule in aqueous solution was analyzed in order to survey its structural behavior free in water and also to rationalize any structural change observed inside the micelle.

The results have shown that the CHAPS hydrophilic "chain" region could be orientated in any direction from the ring group along the trajectory. There are 10 torsional angles that could be defined into this group, not taking into account the amide bond. Among these angles, 3 of them remained in "gauche" conformation most of the simulation time, while the rest adopted a "trans" conformation. In particular the angle around the first bond between the ring group and the chain group is always in "gauche" giving to the molecule a kind of twisted conformation. In Figure 2A we have introduced a cartoon

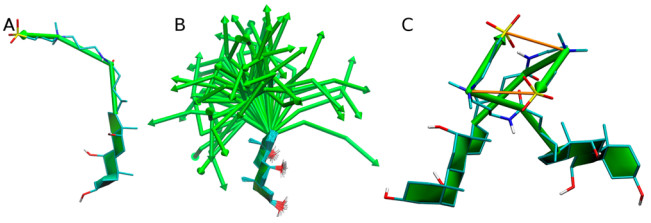

Figure 2. (A) Cartoon representation of the CHAP molecule. (B) The scheme shows the conformational space spanned by the chain portion of a single CHAPS molecule in aqueous solution. The snapshots for the isolated molecule have been fitted in the cholic moiety to evince the orientational freedom of the chain. (C) Initial contacts (salt bridge interaction shown orange lines) between two isolated CHAPS molecules.

representation of the CHAPS molecule that takes into account the above-mentioned features of the structure to simplify its visualization. The rings of the cholic group were rendered with a polyhedron inside of them to ease their visual identification. Furthermore, given the complexity of the micelle organization, it was found useful to represent the chain group with 3 vectors, (i) from the last atom of the cholic group to the carbon atom of the amide group, (ii) from that C atom to the positive nitrogen atom of the dimethylammonium group, and (iii) from that N atom to the sulfur atom in the negatively charged sulfonate group. Figure 2B illustrates the alluded to conformational freedom of the hydrophilic chain region in aqueous solution.

3.2. Molecular Dynamics of Two CHAPS Molecules. The basic idea behind the analysis of this system is to understand the possible initial contacts between 2 molecules and the precursor interactions that lead to the micelle formation. It is known that the thermodynamics of the micellation process involve the hydrophobic effect, the repulsion/attraction between hydrophilic heads, and also the effect of the salt concentration.[32] Therefore, the understanding of the primary contacts between CHAPS molecules and the kind of interactions that stabilize them would improve the knowledge about their aggregation behavior.

The visual analysis of this MD trajectory (and in all MD) showed that the initial approaching between the molecules is guided by the electrostatic attraction between the opposite charge groups in the "chain" moieties (making doubles "salt" bridges as illustrated in Figure 2C). The cholic groups come together after that initial step, in order to hide their hydrophobic faces, and expose their hydrophilic faces to the water. Finally, the last configuration reached by the dimer is the result of a balance between the "chain" and "cholic" interactions, individually. It is worth noting that these features of the dimer are not so obvious as to transfer to aggregates of larger number of members without some kind of frustration in the elemental interactions due to the structure of the CHAPS molecule.

3.3. Molecular Dynamics of CHAPS Micelles. The results for the simulations of micelles containing 4, 6, 8, 10, 12, 14, 16, and 18 molecules were analyzed.

3.3.1. Global Shape of the Micelles. All the simulations starting with 4 to 18 molecules randomly solvated in water result in stable micelles. Furthermore, depending on the number of molecules, the micelle formation occurs between the first 10 ns of simulation for small aggregation number and 25 ns for the larger systems. Only in one of the two systems with 18 molecules it takes almost 80 ns for the equilibration stage to reach the micelle formation, but after this period the aggregate remains stable. Additionally, no dissociation events were found along the simulations on any of the simulated systems once the micelle is already formed. The equilibration of the micelles was monitored by following the temporal evolution of their gyration radii.

3.3.1.1. Gyration Radii. To characterize the overall shape of the micelles containing different numbers of molecules, we used the three instantaneous eigenvalues of the inertia tensor or, what is equivalent, the three radii of gyration. The temporal averages of the homologous radii for micelles of each size along the production stage are presented in Figure 3. The results

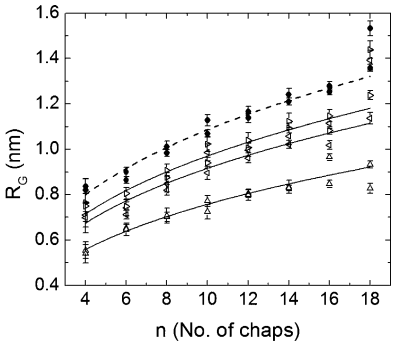

Figure 3. Temporal average of the 3 principal gyration radii as a function of the number of CHAPS molecules in the micelle (different oriented triangles for the 3 values). In filled circles the gyration radii referred to the center of mass. Error bars are calculated from the temporal standard deviation. Also the fitted $N^{1/3}$ curves for each data set are plotted.

show for the micelle of each size two larger and similar radii of gyration, and a smaller and distinct one. These results allow us to characterize the micelles as prolate shaped ellipsoids which agree with the experimental determinations by small angle X-ray scattering (SAXS).[30] The fitted $N^{1/3}$ curve to the dependence of the radii of gyration with the size of the micelles (Figure 3) helps to evince that the asymmetry of the ellipsoids grows with the number of molecules, becoming slightly more elongated.

3.3.1.2. Micelles Size. The principal axis of revolution ellipsoids of uniform mass density that led to these gyration radii are presented in Figure 4 to characterize the micelle sizes. Qin et al.[4] have estimated hydrodynamics radii of the CHAPS micelles from NMR measurements of self-diffusion coefficients. They have found values of 1.5 and 2.7 nm, for concentrations of

dx.doi.org/10.1021/jp501729s | J. Phys. Chem. B XXXX, XXX, XXX−XXX

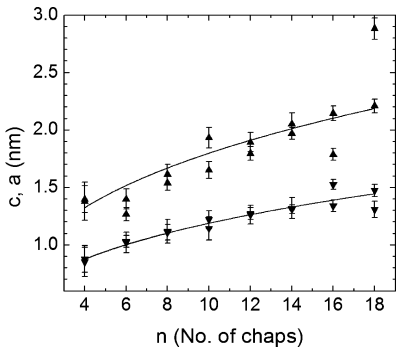

Figure 4. Major (c) and minor (a) principal axes of the constant mass density ellipsoid that reproduce the gyration radii of each simulated micelle as a function of the number of CHAPS molecules. Error bars are calculated from the temporal dispersion of the gyration radii.

20 mM and 80 mM, respectively. Also for 20 mM solutions they characterized the micelle radii by transmission electron microscopy and found a monodisperse distribution with a mean of 1.4 nm. For the higher concentration they found a polydisperse distribution of micelle sizes with mean radius of 2.3 nm. These experimentally estimated radii are within the ranges of those shown in Figure 4.

The relation among the aggregation number of the micelles and the molecular concentration of the surfactant is of central importance to compare experiments and theoretical results. From the SAXS determination of the forward scattering intensity values, micelle aggregation numbers between 12 and 18 molecules have been estimated[30] for concentrations in the range 10 mM to 150 mM. Nevertheless it is difficult to establish a more precise relation among the values determined experimentally and theoretically due to the polydisperse nature of solutions at high concentration. This issue will be addressed anew in the Discussion.

Figure 5 shows the volume of each micelle calculated as the temporal average of those contained in the instantaneous

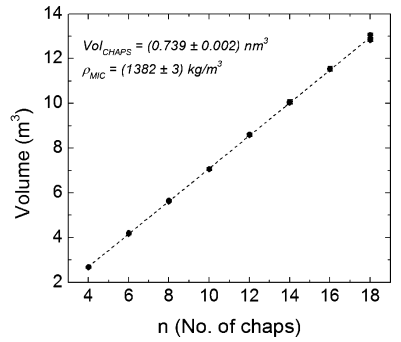

Figure 5. Temporal average of the volume contained in the Connolly or solvent excluded surface as a function of the number of CHAPS molecules for each simulation. Error bars show the dispersion along the simulated time. The linear fitting allows the calculation of the molecular volume and the micelle density.

Connolly or solvent excluded surface of each micelle.[33] Errors bars, which are almost of the size of the symbols, are from the temporal dispersion of this quantity along the production period. The figure evidences the linear growth with the number of CHAPS molecules, and from it one can obtain the effective molecular volume for the CHAPS molecule (V_{CHAPS} = (0.739 ± 0.002) nm^3), and the mass density of the micelle (ρ_{mic} = (1382 ± 3) kg/m^3).

Figure 6 shows a snapshot of the simulation for an equilibrated micelle of 14 molecules to have a more realistic

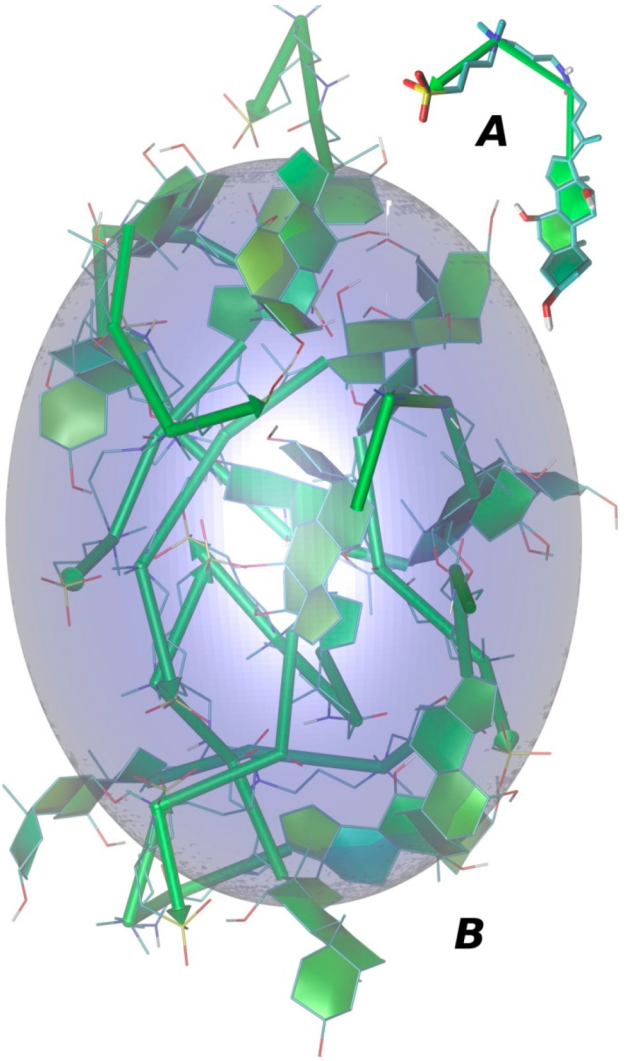

Figure 6. (A) Cartoon representation of the CHAPS molecule used to draw a snapshot of the micelle. (B) Snapshot of the micelle of 14 CHAPS molecules at the end of the production stage. The revolution ellipsoid whose principal axes are presented in Figure 4 for this micelle is shown as a transparent surface.

image of the aggregate shape and structure. This image serves to illustrate the granular heterogeneity in the arrangement of the molecules, despite the rotational properties captured by the gyration radii. The interactions and stabilizing effects that lead to this arrangement are addressed in the following paragraphs. This arrangement of the CHAPS molecules differs from the ones found in micelles of other detergents, which exhibit a central hydrophobic core and an external hydrophilic surface. Nevertheless SAXS results from the work of Lipfert et al.[30] show that CHAPS micelles are singular in their series of 9 studied detergents. They show that the dispersion curve of CHAPS micelles can be modeled by only one homogeneous electronic density ellipsoid. The other detergents in their series require the presence of ellipsoids with a surface shell of higher

dx.doi.org/10.1021/jp501729s | J. Phys. Chem. B XXXX, XXX, XXX−XXX

density to account for the hydrophilic interface that is exposed to the solvent.

3.3.1.3. Electronic Distribution in the Micelles. In Figure 7 we show the electronic radial distribution function (RDF)

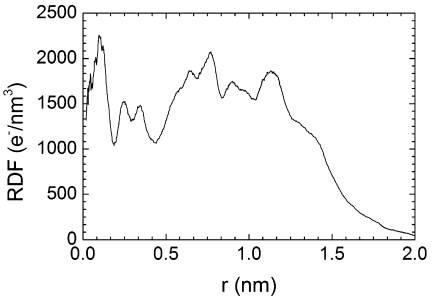

Figure 7. RDF of electrons around the CM of a simulated micelle of 14 CHAPS molecules for the production stage (20 ns).

centered on the center of mass of one simulated micelle with aggregation number of 14. For this micelle, the region between 1.3 and 1.9 nm corresponds to the characteristic size of the micelle (see Figure 4). In this region we observed a smooth decrease in the electronic density. Immediately below this region (r around 1.3 nm), and unlike other detergents, the RDF does not show an electronic concentration substantially higher than that observed deeper inside the micelle. This feature repeats for the other systems. This RDF is calculated from the production stage of 20 ns. The moderate RDF electronic density structure observed in the inner part of the micelle depends on the particular arrangement of each micelle. The implicit ensemble average in the collection of SAXS counts will lead to the disappearance of the structure observed for $r < 1.3$ nm.

3.3.2. Aggregated Structure and Interactions. 3.3.2.1. Radial Distribution Function. Figure 8 shows the RDF of different polar atoms around the sulfonate groups in order to elucidate the electrostatic interactions that are responsible for the heterogeneous arrangement of the micelle. It shows the curves for the micelles with 8, 10, 14, and 16 CHAPS molecules (the curves for all the micelles are presented in the Supporting Information). The curves have been appropriately normalized to make meaningful the comparison among micelles of different number of molecules. Many overall features of the RDFs are similar among the curves corresponding to micelles of different sizes. This fact shows that there are short-range correlations between the various polar groups that are conserved among micelles of different sizes. This feature emphasizes the importance of the electrostatic interactions in the cohesion of CHAPS micelles. The amide N (N^{amide}) of nearby CHAPS molecules are the closest atoms to the sulfur from the sulfonate group together with the oxygen atoms from the cholic−OH, both at peak distances of ∼4 Å. Nevertheless the cumulative RDF indicates that on average only a third of N^{amide} participate in those arrangements while on average almost one of the cholic−OH positions is located at such short distances from sulfur. The charged N (N^+) of neighboring molecules is located, on average, at a distance of ∼4.6 Å from the S, but in this case there is one N^+ atom from a nearby CHAPS molecule close to each sulfonate (similar to the cholic−OH). The "S around S" curves present a broad peak at ∼6 Å that can be associated with the CHAPS molecules whose N^+ atoms interact with the reference sulfur. The cumulative RDFs assign on

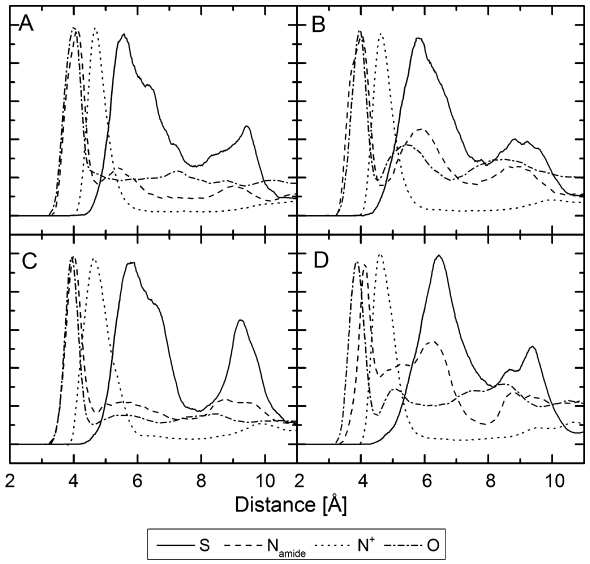

Figure 8. Radial distribution functions (RDFs) for the specified atoms around the sulfur one calculated over the last 20 ns. The RDFs for the micelles with 8 (A), 10 (B), 14 (C), and 16 (D) CHAPS molecules are shown. Appropriately normalized curves are shown to allow meaningful comparisons between micelles of different size. In order to filter the fluctuations due to the bin counts the Savitzky−Golay method for smoothing the curve was used since it is known to preserve the peak shape.[34]

average one neighboring S to this arrangement. In many micelles there is a second peak of the "S around S" RDF at peak distance of ∼9.3 Å that deserves an analysis. By visual inspection one can see that these values of the S−S distance occur when a S atom is located simultaneously close (∼4.5 Å) to the N^{amide} and N^+ of a neighboring CHAPS molecule in agreement with the fact that the cumulative number of the "S around S" RDFs assigned to this peak is one atom on average in almost all systems. Therefore it can be said that the sulfonate group interacts with a neighboring molecule in two alternatives positions: (a) interacting only with the N^+ atom; or (b) interacting simultaneously with N^+ and N^{amide}.

From these results one can conclude that the electrostatic interactions of the sulfonate group with the N^+ and N^{amida} atoms are very important for the formation of the micelle. The salt bridge like interactions (SB) between the N^+ and SO_3 are significant at distances of ∼4.6 Å. Additionally the formation of H-bonds (HB) between the sulfonate oxygens and the OH of cholic moiety or either with the N^{amide} are statistically significant.

Figure 9 shows the temporal average over the last 20 ns of each simulation of the number of salt bridge (SB) and hydrogen bond (HB) interactions excluding those with the water. Both quantities grow with the number of molecules in the micelle, showing the role of these interactions in the stabilization energy of the aggregate. Linear regressions of both sets show that the SB increases with a lower slope.

3.3.2.2. Hydration. Figure 10 shows the temporal average of the solvent accessible surface area (SASA) for micelles of different numbers of molecules to characterize their hydration properties. Additionally, the components of this area that are near polar groups (hydrophilic) and its counterpart that corresponds to the environment of nonpolar atoms (hydrophobic) are also shown in the figure. The linear regressions in Figure 10 for this interval of micelle sizes show that the

dx.doi.org/10.1021/jp501729s | J. Phys. Chem. B XXXX, XXX, XXX−XXX

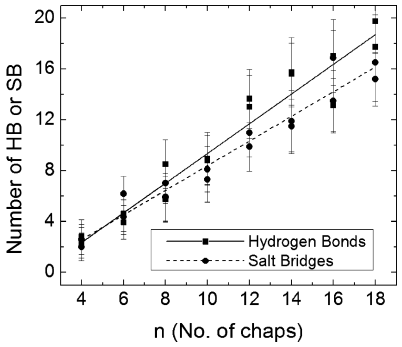

Figure 9. Number of hydrogen bonds (squares) and salt bridges (circles) among the CHAPS molecules as a function of their number in the micelle. The geometric criteria of existence of HB and SB were discussed previously in Methods.

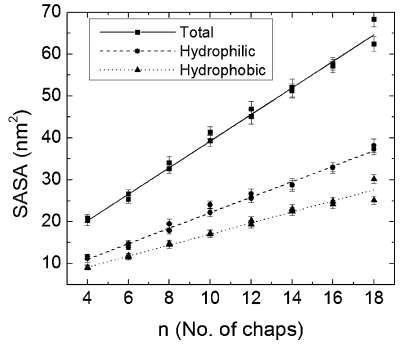

Figure 10. Solvent accessible surface area values as a function of the number of molecules in the micelle. The surface areas that correspond to the polar and nonpolar atoms are also presented.

hydrophobic component of the SASA does not tend to saturate as would be the case if there were a hydrophobic core like in SDS (sodium dodecyl sulfate) or DPC (dodecylphosphocholine) micelles. Unlike these last mentioned molecules which form classical micelles, the SASA of CHAPS micelles show that both of their components grow with their sizes with a rather higher slope in the hydrophilic one. This behavior means that an increasing number of nonpolar groups are exposed to water as the size of the micelles grows. This kind of arrangement could be understood only if there are competing terms in the stabilization energy that counteract these effects like the electrostatic interactions. Due to the peculiar structure of the CHAPS molecule, the arrangement of the aggregate implies that some hydrophobic regions have to be exposed to the solvent. The favorable electrostatic interactions should compensate for that destabilizing contribution.

In order to characterize the nature of the hydration shell of the micelles, we have calculated the quantity of "occluded waters" (Figure 11). These are the water molecules that are in contact with the CHAPS molecules up to a distance of 3 Å and with less than 25% of their solvent accessible surface area (SASA) in contact with other water molecules (in other words, 75% of their SASA is covered or surrounded by CHAPS molecules).

The occluded waters range from 1 to 14 molecules on the different micelles while the contact waters range from 66 to 181 molecules. The position of the occluded water is always close to the hydrophilic groups that remain inside the micelle after its formation. They are found in contact with the oxygen atoms from the sulfate groups or in contact with the hydroxyl group

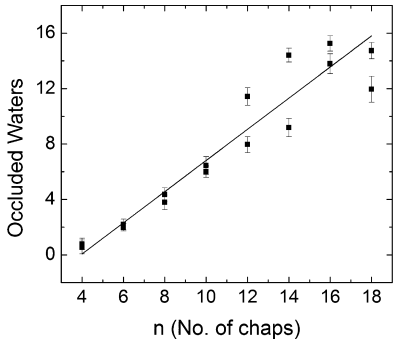

Figure 11. Number of occluded waters as a function of number of CHAPS molecules in the micelles.

on the hydrophilic side of the rings, forming hydrogen bonds with them. No occluded waters were found close to the hydrophobic zone of the molecules.

The number of occluded waters can be thought as a measure of the rugosity of the surface. The SASA area of the micelles roughly doubles the surface of the associated ellipsoid that gives an idea also of the rugosity of the solvent−aggregate interface. It remains to be probed if an increasing dispersion in the number of occluded waters can be associated with some kind of instability of the system.

The residence time of each occluded water molecule was calculated, and it was found that the values are similar to those of other water molecules in contact with the surface of the micelles (around 20 ps). This means that the occluded water molecules are not immobilized inside of a pocket formed in the surface of a micelle but they interchange with other free water molecules.

3.3.2.3. Hydrophobic Stabilization. The visual inspection of the molecular structure of the micelles shows that there are hydrophobic pockets built up by the clustering of the hydrophobic faces of at least 3 CHAPS molecules. An analysis of the RDFs of the methyl groups that protrude from these hydrophobic faces for molecules members of such clusters shows that those arrangements are stable over periods of 20 ns. Figure 12 shows the methyl−methyl RDFs for a CHAPS molecule that form a pocket in the micelle of 14 molecules. It shows the first peak of the curve located at ∼4 Å. The inset corresponds to the cumulative RDF for the same molecule. It

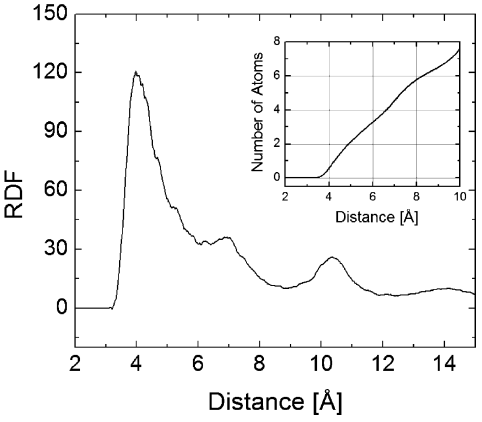

Figure 12. The methyl−methyl RDFs for a CHAPS molecule that forms a pocket in the micelle of 14 molecules. Inset: Cumulative RDF for the same molecule (intramolecular peaks were removed).

dx.doi.org/10.1021/jp501729s | J. Phys. Chem. B XXXX, XXX, XXX−XXX

shows that there are methyl groups from 2 other molecules within a distance of 6.0 Å. Other molecules visually identified as belonging to hydrophobic pockets showed similar results (not shown).

Additionally, we calculated the proximity map of these methyl groups for each of the CHAPS molecules that build up the micelle in order to find out all the hydrophobic micropockets. We calculated the temporal average of the minimum distances between either protruding methyl group of each CHAPS molecule and all the others from the other molecules that form the micelle. These variables were used to quantify the proximity between these hydrophobic groups among different molecules. In Figure 13 this quantity is plotted in a gray scale among all the molecules in a micelle of 12 CHAPS. Since the proximity of these methyl groups is a clue of the formation of a hydrophobic pocket, we can identify the molecules that participate in its building. The diagonal squares obviously are the self-contacts. Each gray square out of the diagonal is a sign of intermolecular proximity between the methyl groups. In the figure it is possible to identify clusters of two, three, and four CHAPS molecules that seem to participate in hydrophobic pockets. The analysis of the same proximity maps for all the micelles (see Supporting Information) allows us to identify the existence of such hydrophobic micropockets in all cases, built up by at least 3 molecules. Noticeably, between 50 and 70% of the molecules in the micelle participate in this kind of hydrophobic pocket.

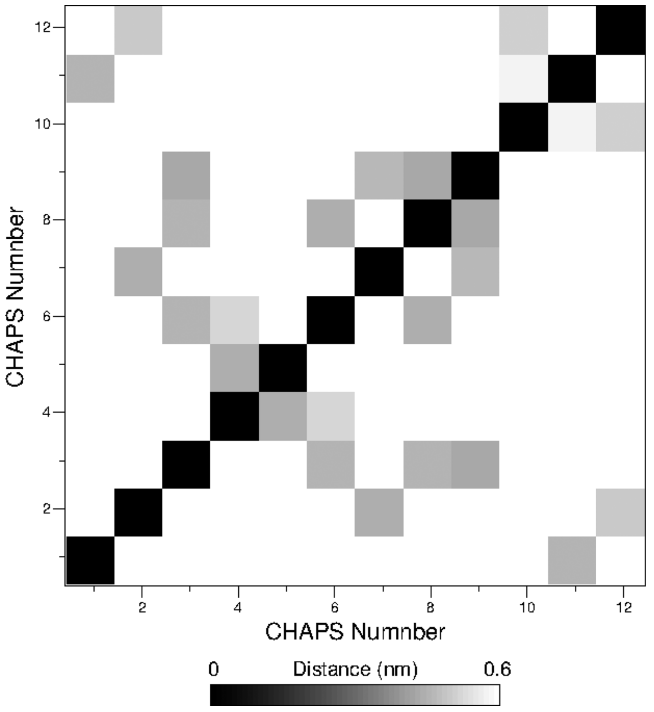

Figure 13. Proximity map among the methyl groups that protrude from the hydrophobic faces of each CHAPS molecule in the 12-membered micelle. The gray scale of the average minimum distance between intermolecular methyl groups goes from 0.0 nm (black) to 0.6 nm (white). The vertical and horizontal axes use a custom index to indentify each CHAPS molecule in the micelle.

3.3.2.4. Simulated NOE Interactions. Qin et al.[4,5] have proposed model structures for the arrangement of CHAPS molecules in micelles based on their 1-D nuclear Overhauser effect (NOESY) measurements. They found evidence of interactions between the methyl groups identified in Figure 14.

We performed a statistical analysis of the proximity of the groups identified by the NOESY experiments in our simulations of micelles of different sizes. We considered that an interaction will be appreciable at a given time if the identified methyl groups are closer than 5.5 Å.[4,5] The analysis was done along the final 20 ns of the production time of each simulation. Results for independent simulations of micelles with the same number of molecules were averaged. The averaged counts, of molecules whose methyl groups of a given kind meet the proximity criteria, are normalized by the number of CHAPS molecules in the micelle. Figure 15 shows these results in a bar

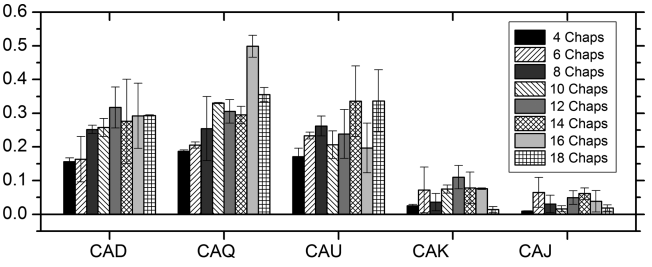

Figure 15. Temporal average percentage of CHAPS molecules on each micelle whose methyl groups are closer than 5.5 Å of the methyl groups of the N^+ atom, and therefore are expected to contribute to the 1-D NOESY spectra obtained by Qin 2011 et al.[4]

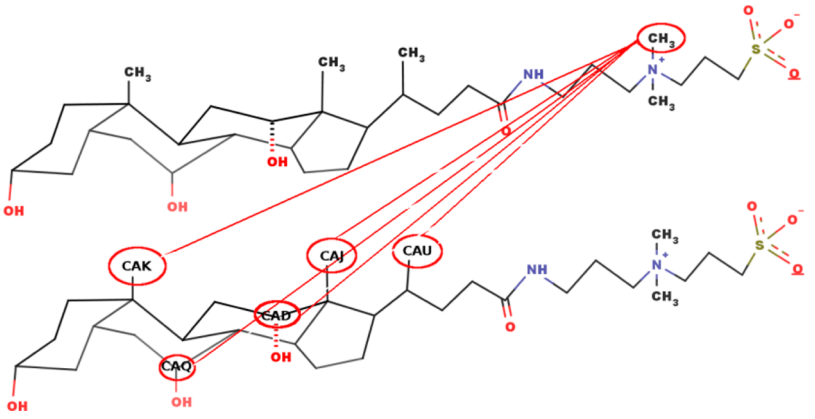

Figure 14. Scheme showing the proximity interactions (<~5.5 Å) that have been detected in the 1-D NOESY spectra of Qin et al.[4,5]

dx.doi.org/10.1021/jp501729s | J. Phys. Chem. B XXXX, XXX, XXX–XXX

graph, for each kind of interaction and micelles of different sizes. As can be seen the different interactions detected by NOESY spectroscopy are present in the structures of the micelles that we have simulated. The detailed analysis of the dependence of the experimental spectra with the concentration of the surfactant is not obvious because, as found by Qin et al.,[4] at high concentrations the solution is polydisperse. Nevertheless it can be observed that the more frequent interactions occur with the methyl groups that are closer to polar groups. In other words the NOE interaction between the N^+ methyl groups and those with a hydrophobic environment (CAK and CAJ, see Figure 14) are less favored.

3.3.3. Rotational Dynamics of the Micelles. 3.3.3.1. Rotational Diffusion. Finally, we have studied the rotational motion of the micelles to obtain the correlation times of their rotational diffusion. These correlation times can be measured by fluorescence anisotropy, or also in some cases by electronic paramagnetic resonance. We have followed the temporal evolution of the spatial orientations of the instantaneous principal axis of inertia of each micelle. We have calculated the self-correlation functions for the axis of inertia that correspond to the larger and smaller eigenvalues. We have used the second order Legendre polynomial as the kernel of the self-correlation functions to obtain both correlation times that correspond to the micelle, that are characterized as a prolate structure ($\tau_\perp$ and $\tau_\parallel$). Figure 16a shows the self-correlation function that corresponds to the principal axis of inertia with the smaller eigenvalue for one of the simulations of a micelle with 14 CHAPS. From the region where the correlation function shows an exponential decay we have obtained the correlation time, in this case $\tau_\perp$. Figure 16b shows the values of correlation times for all the micelles with aggregation numbers between 6 and 18. The correlation times grow with the number of CHAPS molecules as expected, but the $\tau_\perp$ has a slightly larger slope than the $\tau_\parallel$ due to the trend in the shape of the inertia ellipsoid of becoming more elongated with an increasing aggregation number. The annotated dispersions (s_y) in the $\tau_\perp$ and $\tau_\parallel$ are partially related to the distribution of shapes of the micelles with a given aggregation number.

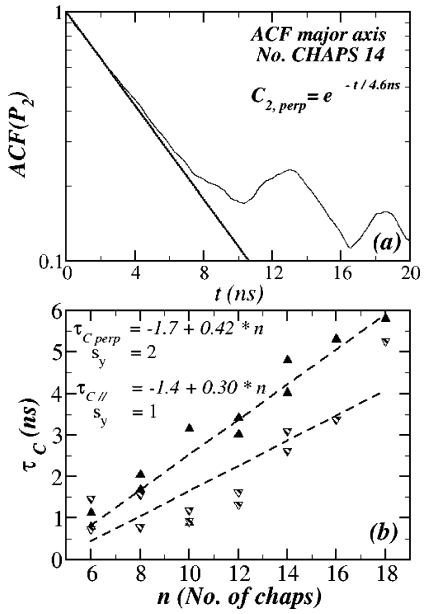

Figure 16. (a) Self-correlation functions of the angle of the instantaneous principal inertia axis that corresponds to the lower eigenvalue using the second order Legendre polynomial as kernel. (b) Correlation times fitted to self-correlations functions in the regions with exponential decay. Filled symbols correspond to the correlation times associated to the lower eigenvalue principal inertia axis ($\tau_\perp$), and hatched symbols to those from the larger eigenvalue principal inertia axis ($\tau_\parallel$). Linear regressions allow the estimation of the values' dispersion.

Gennaro et al.[35] have studied the EPR spectra of solutions of CHAPS molecules at several concentrations, using stearic acid labeled at positions 5, 12, and 16 of the acyl chain. For the case of the spin labeled at site 12 of the acyl chain of the fatty acid they found broader peaks than with the other positions. Additionally, by fitting the spectra of this spin label through the concentration range from 3 mM to 163 mM, they found correlation times for the rotational diffusion of the magnetic orbital that range from 3.15 to 4.85 ns. These values agree with the range of rotational correlation times determined by us (see Figure 16). This fact would mean that an important source of the loss of correlation of the magnetic orbital is the rotational movement of the micelle as a whole, and that the doxyl ring that contributes its unpaired spin is relatively constrained to move in the structure of aggregate.

4. DISCUSSION

Following the initial configuration of the CHAPS molecules homogeneously solvated in the simulation box, and during or after some nanoseconds of the temperature decrease of the annealing stage, most simulated systems show the formation of stable aggregates. No fragmentation events are observed in all the simulated time for all the systems. Along the final 20 ns of the simulations we observe no further changes in the gyration radii or radial distribution functions that may hold a clue about the lack of equilibrium.

The sizes of the simulated systems preclude any possibility to study the thermodynamic equilibrium among micelles of various aggregation numbers and the global concentration of detergent in the solution. Therefore we limited ourselves to study the properties of the micelles of each size and to compare the results with the available experimental data at different detergent concentrations.

The average gyration radii of the different sized micelles show the aggregates as prolate ellipsoids at least from the point of view of their average rotational properties. The sizes of a homogeneous density ellipsoid that are quoted in Figure 4 allow the comparison with some estimation of micelle sizes from experimental results. At low detergent concentration but above the critical micellar one, Qin et al.[4] have determined by TEM images that the solution is monodisperse. This evidence supports the assumption of Lipfert et al.[30] to interpret their SAXS experiments. In that work at 20 mM concentration of detergent the aggregation numbers of micelles are estimated to be 12 from forward scattering intensity. Their fitting of the dispersion curves results in an "apparent gyration radius" of 1.54 nm and a prolate spheroid for the shape of the micelle. Our results also identify the micelle as a prolate ellipsoid for all the aggregation numbers studied. Nevertheless the average gyration radius for the micelles of 12 molecules from our calculations (see Figure 3) is 1.2 nm, slightly lower than the "apparent" value of SAXS. As discussed by Lipfert et al.,[30] the apparent gyration radii from SAXS can overestimate the electronic gyration radii due to the attractive interactions among micelles that are experimentally observed in CHAPS

dx.doi.org/10.1021/jp501729s | J. Phys. Chem. B XXXX, XXX, XXX−XXX

solutions. The principal axis of the ellipsoid for $n = 12$ are $a = b = 1.3$ nm and $c = 1.9$ nm. Qin et al.[4] do not report prolate shapes in their TEM images of supported dried micelles and give a value for the radius of 1.4 nm. In the same work they estimate hydrodynamic radius of the micelle by NMR of solutions of 20 mM CHAPS and give a value of 1.5 nm. Our result for the radius of a sphere, with the same volume as the ellipsoid of our simulations, is 1.47 nm, in agreement with those data. The ratio of the principal axis of the ellipsoid for $n = 12$ is ~1.46, which contrasts with the remarkable value of 2.95 reported by Lipfert et al.[30] for a 25 mM solution.

For concentrations of 80 mM of CHAPS, Qin et al.[4] characterize the solution as polydisperse (inhomogeneous) based on their TEM images, with a broad distribution of micelle sizes that has a mean of 2.3 nm. Their results from hydrodynamic radius estimations give a value of 2.7 nm. The SAXS results of Lipfert et al.[30] give an estimation of $n = 17$ for the aggregation number at 80 mM solution. It must be taken into account that for this case the assumption of the monodisperse nature of the solution is questionable. Nevertheless, from our fitting of the principal axis of the ellipsoids, the largest value for a micelle of 18 molecules gives 2.2 nm, close to the mean value of TEM images. Qin et al.[4] argue that the hydrodynamic radius obtained by NMR from self-diffusion measurements can be overestimated due to the fact that the micelle movement is accompanied by a hydration shell at variance with TEM images that are from dried micelles.

It is worth noticing that our determination of the CHAPS molecular volume and density in micelles is novel and useful for the extraction of other parameters from SAXS experiments.

The obtained results suggest that the relationship between the electrostatic and hydrophobic interactions plays an important role not only in the stabilization of the micelles but also into their formation with a particular number of molecules. During the formation and stabilization of the micelles, charge pairing interactions among the zwitterionic tails and also with the OH of the ring moiety occurs (see RDFs in Figure 8, and the number of SB and HB in Figure 9). Additional stabilization comes due to the clustering of the steroidal rings in small hydrophobic pockets of 3−4 molecules (see RDF and proximity plot in Figures 12 and 13). These interactions lead the aggregates to have a "micellar heterogeneity" characterized by a grainlike microstructure (very different from the micelles of other compounds) that is related to the optimization of the free energy. These features agree with the SAXS results[30] that model the dispersion curves with only one constant electronic density ellipsoid (see RDF of electronic density at Figure 7) at variance with other detergents. The arrangements of the CHAPS molecules into the micelles, that we found, are less symmetric than those proposed by Qin et al.[4,5] to account for their spectroscopic data. We have shown that the NMR−NOE interactions measured by Qin et al.[4] are also present in our models of the micelles. Kawamura et al.[36] have proposed structural models for the aggregation of bile salt molecules based in their EPR results. Their model of bile salt micelles shows also high symmetry at variance with our simulations. Nevertheless the interpretation of EPR results from a spin label demands to know the environment in which this molecule is attached to the micelle. Therefore we considered it highly speculative to conclude if the results of our simulation agree or not with that experimental evidence.

The surfaces of all micelles with different aggregation numbers present one or more patches of zwitterionic tails favored by the electrostatic interactions and the flexibility of this moiety (Figures 6 and 7). Additionally some nonpolar groups are exposed to the solvent as shown in Figure 6. At variance with other amphiphilic molecules, CHAPS has a steroidal moiety with a nonpolar convex face, a partially polar concave side, and a one-dimensional zwitterionic tail. The peculiar polar groups distribution in the CHAPS molecule lead to this kind of heterogeneous structure that is the result of the frustration between competing interactions. The surface of the micelles has a high degree of rugosity as shown by our results of SASA (Figure 10) and occluded water counts (Figure 11). Additionally, hydrophobic pockets formed by at least 3 CHAPS molecules were found inside each micelle, and the number of these pockets increases with the number of monomers (see proximity maps in the Supporting Information).

The study of the rotational properties of the micelles and the determination of rotational diffusion times allow for the use of other experimental tools to explore the properties of these aggregates. We found that the correlation times in our determinations are similar to those found for the movement of the magnetic orbital of spin labels inserted in CHAPS micelles measured by EPR.[35] This fact means that the rotation of the micelle as a whole is observable in the line shapes of the EPR spectra.

5. CONCLUSIONS

This work has presented a force field parametrization developed for molecular dynamics simulation of CHAPS molecules. To our best knowledge, it is the first force field based simulation of the structural properties of CHAPS micelles in water.

As already discussed above, our results agree with most of the experimental information available today for this system. They allow the obtaining of an ab initio atomistic structure of the micelles, to predict their properties, and to investigate the details of the interactions that stabilize and lead to the formation of the aggregates. This is relevant in the present case since the structure and charge distribution of the CHAPS molecule, at variance with other detergents, make it difficult to build model micelles by thumb rules.

All the results demonstrate that molecular dynamics simulations are a very good tool to study these types of systems. The following efforts would be directed to perform simulations of similar systems with the spin labels used in EPR experiments.

Nevertheless, it is worth noting that, in phase with the advance in computing power, a continuous improvement of the force field parameters of this types of molecule and the development of new ones should be done in order to improve the perspectives associated with the simulation of micellar systems formed by different molecules since this is a very promising field.

■ ASSOCIATED CONTENT

Supporting Information

The force field parameters and the contacts maps for all the systems are included (Figures S1 to S8). This material is available free of charge via the Internet at http://pubs.acs.org.

■ AUTHOR INFORMATION

Corresponding Author

*E-mail: herrerafer@gmail.com. Phone: +54 342 4575213.

Notes

The authors declare no competing financial interest.

■ ACKNOWLEDGMENTS

We acknowledge the use of the computational facilities of the FaCAP (Facilidad de Computación de Alta Performance) of the Facultad de Bioquímica y Ciencias Biológicas, Universidad Nacional del Litoral. The present work is funded by grants of CONICET and Universidad Nacional del Litoral. F.E.H. and D.E.R. are staff members of the Consejo Nacional de Investigaciones Científicas y Técnicas (CONICET). We acknowledge useful discussions with A. M. Gennaro and P. Rodi from the EPR group.

■ REFERENCES

(1) Lichtenberg, D.; Robson, R. J.; Dennis, E. A. Solubilization of Phospholipids by Detergents. Structural and Kinetic Aspects. *Biochim. Biophys. Acta* **1983**, *737*, 285−304.

(2) Rodi, P. M.; Trucco, V. M.; Gennaro, A. M. Factors Determining Detergent Resistance of Erythrocyte Membranes. *Biophys. Chem.* **2008**, *135*, 14−18.

(3) Hjelmeland, L. M. A Nondenaturing Zwitterionic Detergent for Membrane Biochemistry: Design and Synthesis. *Proc. Natl. Acad. Sci. U.S.A.* **1980**, *77*, 6368−6370.

(4) Qin, X.; Liu, M.; Yang, D.; Zhang, X. Concentration-Dependent Aggregation of CHAPS Investigated by NMR Spectroscopy. *J. Phys. Chem. B* **2010**, *114*, 3863−3868.

(5) Qin, X.; Liu, M.; Zhang, X.; Yang, D. Proton NMR Based Investigation of the Effects of Temperature and NaCl on Micellar Properties of CHAPS. *J. Phys. Chem. B* **2011**, *115*, 1991−1998.

(6) Giacomelli, C. E.; Vermeer, A. W. P.; Norde, W. Micellization and Adsorption Characteristics of CHAPS. *Langmuir* **2000**, *16*, 4853−4858.

(7) Funasaki, N.; Fukuba, M.; Hattori, T.; Ishikawa, S.; Okuno, T.; Hirota, S. Micelle Formation of Bile Salts and Zwitterionic Derivative As Studied by Two-Dimensional NMR Spectroscopy. *Chem. Phys. Lipids* **2006**, *142*, 43−57.

(8) Bogusz, S.; Venable, R. M.; Pastor, R. W. Molecular Dynamics Simulations of Octyl Glucoside Micelles: Structural Properties. *J. Phys. Chem. B* **2000**, *104*, 5462−5470.

(9) Bogusz, S.; Venable, R. M.; Pastor, R. W. Molecular Dynamics Simulations of Octyl Glucoside Micelles: Dynamics Properties. *J. Phys. Chem. B* **2001**, *105*, 8312−8321.

(10) Bruce, C. D.; Berkowitz, M. L.; Perera, L.; Forbes, M. D. E. Molecular Dynamics Simulation of Sodium Dodecyl Sulfate Micelle in Water: Micellar Structural Characteristics and Counterion Distribution. *J. Phys. Chem. B* **2002**, *106*, 3788−3793.

(11) Marrink, S. J.; Mark, A. E. Molecular Dynamics Simulations of Mixed Micelles Modeling Human Bile. *Biochemistry* **2002**, *41*, 5375−5382.

(12) Warren, D. B.; Chalmers, D. K.; Hutchison, K.; Dang, W.; Pouton, C. W. Molecular Dynamics Simulations of Spontaneous Bile Salt Aggregation. *Colloids Surf., A* **2006**, *280*, 182−193.

(13) Bockmann, R. A.; Caflisch, A. Spontaneous Formation of Detergent Micelles Around the Outer Membrane Protein OmpX. *Biophys. J.* **2005**, *88*, 3191−3204.

(14) Di Giampaolo, A.; Cerichelli, G.; Chiarini, M.; Daidone, I.; Aschi, M. Structure and Solvation Properties of Aqueous Sulfobetaine Micelles in the Presence of Organic Spin Probes: a Molecular Dynamics Simulation Study. *Struct. Chem.* **2013**, *24*, 945−953.

(15) Lee, S.; Tran, A.; Allsopp, M.; Lim, J. B.; Hénin, J.; Klauda, J. B. CHARMM36 United Atom Chain Model for Lipids and Surfactants. *J. Phys. Chem. B* **2014**, *118*, 547−56.

(16) Berger, O.; Edholm, O.; Jahnig, F. Molecular Dynamics Simulations of a Fluid Bilayer of Dipalmitoylphosphatidylcholine at Full Hydration, Constant Pressure, and Constant Temperature. *Biophys. J.* **1997**, *72*, 2002−2013.

(17) Oostenbrink, C.; Soares, T. A.; van der Vegt, N. F.; van Gunsteren, W. F. Validation of the 53A6 GROMOS Force Field. *Eur. Biophys. J.* **2005**, *34*, 273−284.

(18) Pandit, S. A.; Chiu, S. W.; Jakobsson, E.; Grama, A.; Scott, H. L. Cholesterol Packing Around Lipids with Saturated and Unsaturated Chains: A Simulation Study. *Langmuir* **2008**, *24*, 6858−6865.

(19) Schuttelkopf, A. W.; van Aalten, D. M. PRODRG: a Tool for High-Throughput Crystallography of Protein-Ligand Complexes. *Acta Crystallogr., Sect. D: Biol. Crystallogr.* **2004**, *60*, 1355−1363.

(20) Malde, A. K.; Zuo, L.; Breeze, M.; Stroet, M.; Poger, D.; Nair, P. C.; Geerke, D. P.; Stougie, L.; Klau, G. W. An Automated Force Field Topology Builder (ATB) and Repository: Version 1.0. *J. Chem. Theory Comput.* **2011**, *7*, 4026−4073.

(21) Canzar, S.; El-Kebir, M.; Pool, R.; Elbassioni, K.; Mark, A. E.; Geerke, D. P.; Stougie, L.; Klau, G. W. Charge Group Partitioning in Biomolecular Simulation. *J. Comput. Biol.* **2013**, *20*, 188−198.

(22) Berendsen, H. J. C.; van-der Spoel, D.; van Drunen, R. GROMACS: A Message-Passing Parallel Molecular Dynamics Implementation. *Comput. Phys. Commun.* **1995**, *91*, 43−56.

(23) Van Der Spoel, D.; Lindahl, E.; Hess, B.; Groenhof, G.; Mark, A. E.; Berendsen, H. J. GROMACS: Fast, Flexible, and Free. *J. Comput. Chem.* **2005**, *26*, 1701−1718.

(24) Pronk, S.; Pall, S.; Schulz, R.; Larsson, P.; Bjelkmar, P.; Apostolov, R.; Shirts, M. R.; Smith, J. C.; Kasson, P. M.; Van Der Spoel, D.; et al. GROMACS 4.5: A High-Throughput and Highly Parallel Open Source Molecular Simulation Toolkit. *Bioinformatics* **2013**, *29*, 845−854.

(25) Darden, T.; York, D.; Pedersen, L. G. Particle Mesh Ewald: An Nlog(N) Method for Ewald Sums in Large Systems. *J. Chem. Phys.* **1993**, *98*, 10089−10092.

(26) Berendsen, H. J.; Grigera, J. R.; Straatsma, T. P. The Missing Term in Effective Pair Potentials. *J. Phys. Chem.* **1987**, *91*, 6269−6271.

(27) Hess, B.; Bekker, H.; Berendsen, H. J.; Fraaije, J. LINCS: A Linear Constraint Solver for Molecular Simulations. *J. Comput. Chem.* **1998**, *18*, 1463−1472.

(28) Miyamoto, S.; Kollman, P. A. Settle: An Analytical Version of the SHAKE and RATTLE Algorithm for Rigid Water Models. *J. Comput. Chem.* **1992**, *13*, 952−962.

(29) Berendsen, H. J. C.; Postma, J. P. M.; van Gunsteren, W. F.; Hermans, J. Interaction Models for Water in Relation to Protein Hydration. In *Intermolecular Forces*; Pullman, B., Ed.; Reidel: Dordrecht, Netherlands, 1981; pp 331−342.

(30) Lipfert, J.; Columbus, L.; Chu, V. B.; Lesley, S. A.; Doniach, S. Size and Shape of Detergent Micelles Determined by Small-Angle X-Ray Scattering. *J. Phys. Chem. B* **2007**, *111*, 12427−12438.

(31) Humphrey, W.; Dalke, A.; Schulten, K. VMD - Visual Molecular Dynamics. *J. Mol. Graphics* **1996**, *14*, 33−38.

(32) Butt, H. J.; Graff, K.; Kappl, M. *Physics and Chemistry of Interfaces*; Wiley-VCH: Weinhein, 2006; pp 269−277.

(33) Sanner, M. F.; Olson, A. J.; Spehner, J. C. Reduced Surface: An Efficient Way to Compute Molecular Surfaces. *Biopolymers* **1996**, *38*, 305−320.

(34) Savitzky, A.; Golay, M. J. E. Smoothing and Differentiation of Data by Simplified Least Squares Procedures. *Anal. Chem.* **1964**, *36*, 1627−1639.

(35) Rodi, P. M.; Bocco Gianello M. D.; Gennaro A. M. Insights About CHAPS Aggregation Obtained by Spin Label EPR Spectroscopy. *Personal communication.*

(36) Kawamura, H.; Murata, Y.; Yamaguchi, T.; Igimi, H.; Tanaka, M.; Sugihara, G.; Kratohvil, P. Spin-Label Studies of Bile Salt Micelles. *J. Phys. Chem.* **1989**, *93*, 3321−3326.